X-band PN Delta DOR Signal Design and Implementation on the JPL Iris Transponder

Zaid J. Towfic, Thaddaeus J. Voss, Mazen M. Shihabi, and James S. Border
Jet Propulsion Laboratory, California Institute of Technology
4800 Oak Grove Dr.
Pasadena, CA 91109
818-354-3345
{Zaid.J.Towfic, Thaddaeus.J.Voss, Mazen.M.Shihabi, James.S.Border}@jpl.nasa.gov

Abstract—**This paper describes the design and implementation of the Pseudorandom-Noise (PN) Delta Differential One-way Ranging (DDOR) signal format on the JPL Iris Cubesat Software Defined Radio. The Iris radio is now in-flight use in Deep Space onboard the MARCO spacecraft and will soon be utilized to multiple EM-1 missions. The spread spectrum Delta DOR format enables more accurate differential ranging measurements over the classical DOR tone format, and it is applicable to deep space missions that require accurate navigation or require accurate angular position measurements for another purpose such as determining the ephemeris of a planet or small body. The classical Delta-DOR technique makes time delay measurements of spacecraft and quasar signals to determine spacecraft angular position in the radio reference frame defined by the quasar coordinates. The measurement system is configured to provide common-mode error cancellation as nearly as possible.**

In the PN DOR mode, instead of a spacecraft modulating their downlink, with a sinusoidal signal, referred to as a DOR tone as done in the classical DOR mode, the sinusoidal tone is replaced with a spread spectrum signal. Using a spread spectrum DOR signal instead of a DOR tone enables cancellation of effects due to phase dispersion across the channels used to record quasar signals. This error source, referred to as phase dispersion or phase ripple, is currently the dominant measurement error for the classical DOR format. PN spreading will improve on classical DOR performance accuracy because by choosing the PN spreading code and shaping filter carefully, the spacecraft signal can be made to closely resemble the quasar signal resulting in reduction of the Delta-DOR error due to phase dispersion by 80% to 90% over the classical DDOR approach.

The article will describe the choice of a Gold code sequence that possesses good autocorrelation properties as well as excellent cross-correlation properties that was used to spread the DOR tone, and the choice of root-raised-cosine (RRC) chip-shaping filter to reduce the amount of excess-bandwidth of the output waveform. The paper will also describe the path that was taken for the FPGA implementation on the Iris radio including a Simulink model of the PN DDOR module that is used for automatic HDL code generation. This module was then integrated into the Iris firmware and verified.

Future work includes the integration of the designed subsystem into the Universal Space Transponder and extension of the derived waveform to the KA-band. We hope that the outlined PN DDOR implementation can be integrated into an upcoming mission that utilizes the Iris radio (such as EM-1 missions).

TABLE OF CONTENTS

1. INTRODUCTION

The Delta Differential One-way Ranging (DDOR) technique makes time delay measurements of spacecraft and quasar signals to determine spacecraft angular position in the radio reference frame defined by the quasar coordinates. These measurements are often critical to deep space missions requiring accurate navigation, such as a spacecraft on a direct trajectory from Earth to a landing on Mars. The measurement system is configured to provide common-mode error cancellation as nearly as possible. The "Delta" delay between spacecraft and quasar measurements has high accuracy, even as effects such as station clock offsets cause sizable errors in the spacecraft measurements alone.

Improved DDOR accuracy remains a goal, to meet more stringent navigation requirements, and enable previously unattainable navigation capability.

In current usage, spacecraft modulate their downlink with a sinusoidal signal, referred to as a DOR tone, to provide a wide spanned bandwidth that enables a precise group delay measurement. This wide spanned bandwidth is especially needed to make precise group delay measurements of weak quasar signals. For X-band downlinks, a DOR subcarrier frequency of about 19 MHz is typical, as this is within the spectrum allocation for deep space research at X-band. Quasar signals are typically recorded in channels with bandwidth of 8MHz.

The research was carried out at the Jet Propulsion Laboratory, California Institute of Technology, under a contract with the National Aeronautics and Space Administration.

During a DDOR measurement session, quasars that are angularly close to the spacecraft are simultaneously observed, to provide common-mode cancellation of common-mode effects, including station coordinate errors and media calibration errors. Antennas slew back and forth between spacecraft and quasars to provide common-mode cancellation of temporal effects, including station clock drifts. Quasar signals are recorded in channels centered on the received frequencies of spacecraft DOR tones to provide common-mode cancellation of clock offsets and station group delays. However, the current architecture does not provide cancellation of effects due to phase dispersion across the channels used to record quasar signals. This error source, referred to as phase dispersion or phase ripple, is often the dominant measurement error for DDOR. The per channel phase error is typically in the range of 0.2 to 0.5 degrees [1].

Receiving systems used for deep space communications are among the most sensitive and tightly specified radio systems in existence. Even so, phase linearity across channels of several MHz bandwidth, at the level of a fraction of a degree of phase, cannot be assumed. But, common-mode cancellation of phase dispersion effects is possible for DDOR by using a wideband signal with noise-like features---i.e., similar to the quasar signal This can be artificially done with the use of pseudo-noise sequences.

Consider Figure 1. The two spectra on the left-hand side are data from an actual DDOR measurement. The top-left figure is the spectrum of receiver noise in a channel, with the flat quasar signal buried in the noise. The bottom-left figure is the spectrum of a spacecraft DOR tone in a noise channel. The two spectra on the right-hand side are theoretical spectra of a DOR tone spread with a PN code. The top-right figure is the spectrum of a PN code with rectangular chips. The bottom-right figure is the spectrum of a PN code with shaped chips.

By choosing the PN spreading code and shaping filter carefully, the spacecraft signal can closely resemble the quasar signal. Reduction of the DDOR error due to phase dispersion can be reduced by 80% to 90%.

While PN spreading will improve DDOR performance at X-band, even more improvement is possible at Ka-band. Since quasar flux is lower at Ka-band and ground station system noise temperature is higher, more bandwidth is required for group delay measurements at Ka-band. This improves on the precision of quasar group delay measurements at X-band. A DOR subcarrier frequency of about 160 MHz is envisaged for Ka-band with a flat spectrum signal filling a bandwidth of about 32 MHz centered on the subcarrier sidebands.

In the next section, we will discuss the general requirements of the PN DDOR waveform. Following this, we will discuss how the structure of the waveform will be influenced by these requirements and appropriate waveform parameters will be selected. We will then outline the fixed-point design of the PN DDOR module and discuss its integration into the JPL Iris cubesat radio firmware. The Iris radio is now in-flight use in Deep Space onboard the Mars Cube One spacecraft and will soon be utilized to multiple EM-1 missions [2]-[3].

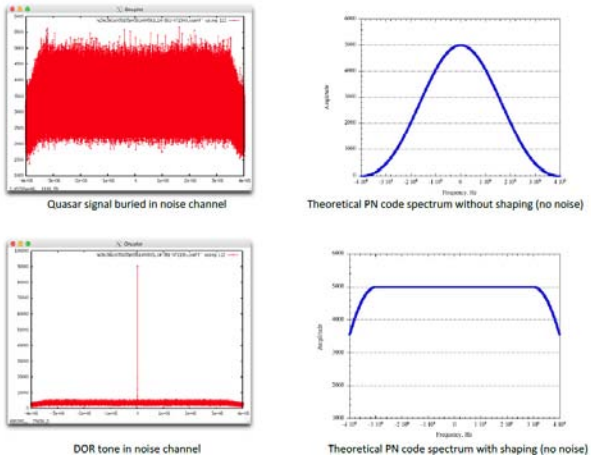

Figure 1. The two spectra on the left-hand side are data from an actual DDOR measurement. The two spectra on the right-hand side are theoretical spectra of a DOR tone spread with a PN code.

2. X-Band PN Delta DOR Iris Design

The key PN DDOR derived design parameters for the X-Band Pseudo Noise (PN) Delta Differenced One-way Ranging (DDOR) implementation, as discussed in the last section, are the following:

- The two classical DDOR 19 MHz-offset-from-carrier tones are each replaced with a 8MHz-bandwidth signal that more closely resembles the quasar signal.
- Code period > 1ms in order to maximize the integration time for the DDOR PN sequence correlation (increase SNR).
- Code must have good autocorrelation properties in order to improve the time resolution during the DDOR processing.
- It is also desirable that the code have good cross-correlation properties.
- A small roll-off factor of < 0.3 must be used on the pulse-shaping filter in order to make the spectrum as flat as possible in the pass-band, with a span of 16-chips.

In the next sections, we will determine a suitable code and chip-shaping filter to be used on the Iris processor to satisfy the above requirements. First, we will determine the appropriate code rate in chips per second and the associated chip-shaping-filter, and then we will determine the code structure and primitive polynomials associated with the chosen code.

Code Rate

Given the requirements, and the fact that the chips are going to be filtered by a root-raised-cosine (RRC) filter [4], we will observe that the following relationship between the output bandwidth of the filter and the input chip-rate will hold:

$$BW = R_C(1+\beta)$$

Where β denotes the roll-off factor of the filter. Clearly, we will always have that the inequality:

$$R_C \leq BW$$

will be valid for any $\beta \geq 0$. Now, we know that the chip rate must be an integer fraction of the FPGA clock frequency:

$$R_C = \frac{F_{\text{FPGA}}}{K}$$

for some integer $K \in \mathbb{Z}$, which is the root-raised cosine interpolation ratio. Substituting the relationship of R_C into the bandwidth equation, we obtain:

$$BW = \frac{F_{FPGA}}{K}(1+\beta)$$

This equation has two degrees of freedom (K and β) and two already-determined constants (BW and F_{FPGA}). It is possible to create a table of possible choices for K and β and pick an appropriate choice that satisfies the constraints. This table is generated by sweeping K across the integers and solving for the appropriate β once we substitute $BW = 8\text{MHz}$ and the appropriate FPGA clock frequency for F_{FPGA}.

It is important to note that a higher roll-off factor will allow the output signal to have a sharper histogram, and thus allow the design to allocate more power to the PN sequence than the carrier since a higher roll-off factor will reduce the tail of the filtered PN output distribution and thus allow the gain to be increased further than in the case of a lower roll-off factor (as long as the fact that a wider transition band will appear within the 8MHz target bandwidth can be tolerated).

Code Length

The driving requirement behind the code length is the fact that the code period must be at least 1ms. Considering the code rate obtained in the last section, we have that the code length is related to the code period via the following equality:

$$2^N - 1 = T_c \cdot R_c$$

where T_c denotes the code period in seconds, $2^N - 1$ denotes the code length in chips. Given our requirement that $T_c > 1\text{ms}$, we have:

$$T_c = \frac{2^N - 1}{R_c} > 1\text{ms}$$

It is possible to obtain a sufficient condition on the code period via the inequality $R_C \leq BW$. This gives:

$$T_c = \frac{2^N - 1}{R_c} \geq \frac{2^N - 1}{BW} = \frac{2^N - 1}{8\text{MHz}} > 1\text{ms}$$

which implies that:

$$N > 12.966$$

where $N \in \mathbb{Z}$, since it represents the number of bits in the linear feedback shift register (LFSR). Thus, we have that the above inequality is automatically satisfied when

$$N \geq 13$$

which implies that the code length must satisfy

$$2^N - 1 \geq 8191$$

Observe that in this case, the code length was completely determined by the bandwidth and the code period requirement, and does not explicitly depend on the code rate.

Primitive Polynomial Pairs

Given the code length obtained, we must now obtain the actual PN sequence to be used in the Delta DOR tone spreading. There are generally two PN sequences that are considered for such an application, namely:

- Maximal Length Sequences (M-sequence)
- Gold Codes

M-sequences have very good autocorrelation properties, meaning that the autocorrelation plot of the M-sequence against itself will yield a very high peak at the origin (in fact, the peak in the absence of noise will be the length of sequence) and very low off-center correlations. However, the M-sequence has a drawback in that it is not immediately very well suited for cross-correlation against *other* M-sequences (e.g., in the case of direct sequence spread spectrum multi-user applications such as when multiple spacecraft share the same downlink radio-frequency channel). For the purpose of mitigating this drawback, the Gold Codes were introduced [5]. These codes utilize very specifically picked M-sequence polynomials that are exclusive-or'd (XOR) together to produce up to $2^N - 1$ sequences that exhibit good cross-correlation performance against one another and good auto-correlation performance by themselves. The drawback, however, is the added complexity to implement them (essentially the implementation of two M-sequences) and a slightly worse auto-correlation performance than M-sequences. To see this, we picked a Gold sequence with $N = 11$ as well as an M-sequence of the same length. The autocorrelation performance is illustrated in Figure 1. We observe that while both sequences exhibit good pseudo-random behavior, the M-sequence autocorrelation is slightly better behaved than that of the Gold sequence. However, good cross-correlation performance is desired if different codes will be used for different nearby spacecraft (such as adjacent CubeSats).

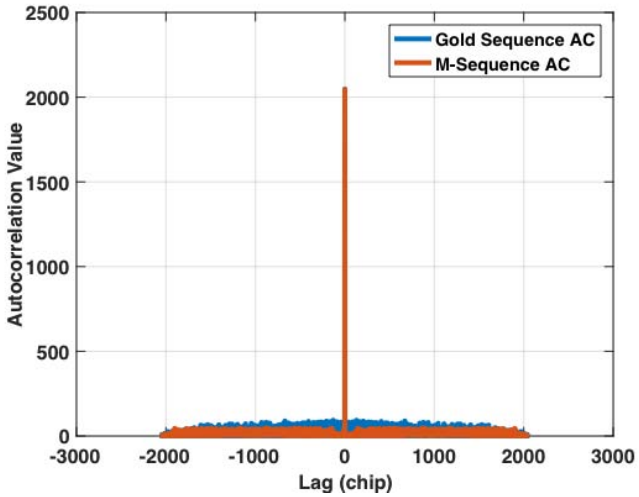

Figure 1. Autocorrelation performance of a M-sequence and a Gold sequence.

Nevertheless, it was determined that the implementation shall utilize a Gold sequence with $N \geq 13$ as outlined in the previous section, to allow for the possibility of overlapping frequency channels for ranging. The next task is to pick a "primitive polynomial pair", i.e., the generating polynomial of two M-sequences that are specifically chosen according to the following theorem [5]:

Theorem

Let f_1 and f_t be a preferred pair of primitive polynomials of degree N whose corresponding shift registers generate maximal linear sequences of period $2^N - 1$ and whose cross-correlation function θ satisfies the inequality.

$$|\theta| \leq \begin{cases} 2^{(N+1)/2} + 1 & \text{for } N \text{ odd} \\ 2^{(N+2)/2} + 1 & \text{for } N \text{ even } N \neq mod\ 4 \end{cases}$$

Then the shift register corresponding to the product polynomial $f_1 \cdot f_t$ will generate $2^N + 1$ different sequences each period $2^N - 1$ and such that the cross-correlation function θ of any pair of such sequences satisfies the above inequality.

For our case, it is ideal to pick an odd $N \geq 13$ and thus the first line of the correlation constraint is to be tested. A table of all possible M-sequence generating polynomials for any N can be found in [6] (it should be noted that reversing the order of the taps in any of the tables will result in another valid M-sequence generator polynomial as well, but those reversed taps are not listed in the table). By verifying the inequality in the Theorem, a valid preferred polynomial pair for a given odd N can be found.

The structure of the Gold code generation is listed in Figure 2. The initial states are stored in the delay elements of the block diagram. The top PN sequence generator creates an M-sequence with one of the two primitive polynomials, $p(z)$, found through verifying the theorem, while the bottom PN sequence generator creates an M-sequence with the second primitive polynomial, $q(z)$, also found by verifying the theorem. The two sequences are then combined via an exclusive or (XOR) operation. The resulting PN sequence is a Gold sequence due to the choice of $p(z)$ and $q(z)$. The final block converts 0/+1 binary PN sequence to a -1/+1 bipolar sequence.

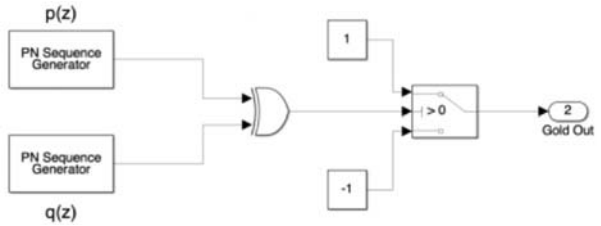

Figure 2. The Gold code generation block diagram.

Chip Shaping Filter

The chip shaping filter limits the bandwidth of the PN sequence, but increases the dynamic range of the time-domain signal. Based on the discussion in the last section, a roll-off factor that is related to the FPGA clock frequency and the samples per chip (K) is determined. The final parameter of the RRC filter is the filter span. For this, the design parameters required the use of a 16 chip span. Higher spans help in flattening the passband frequency response while suppressing the stop-band further. To see this, we consider 2, 4, 8, and 16 chip span RRC filters in Figure 3. The penalty of using higher spans is that longer filters require higher complexity in the FPGA implementation (more multipliers).

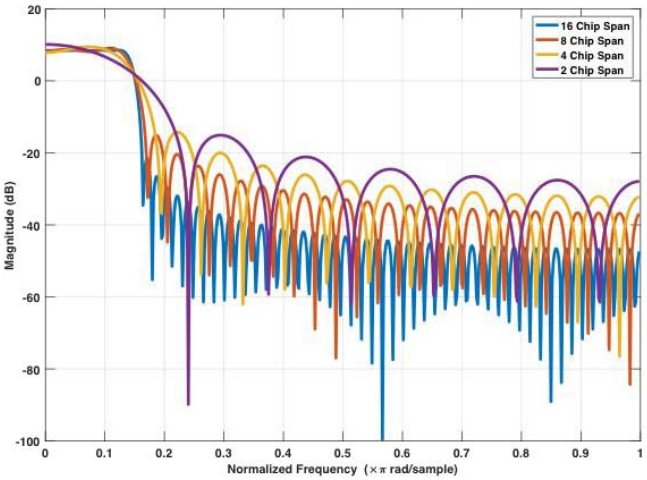

Figure 3. RRC filters with different spans. Higher spans suppress the stop-band further and flatten the pass-band.

3. X-BAND IRIS IMPLEMENTATION

In terms of the implementation of the PN generator, the traditional 19MHz subcarrier generation is assumed to be present in the radio HDL code (such as Iris). However, the Gold code implementation, as well as the RRC filter must be implemented in fixed-point. This was done using Simulink and its built-in functions including Gold Sequence Generator and RRC transmit filter. Both of these blocks are compatible with Simulink's HDL coder which can generate Verilog/VHDL code automatically from the Simulink block diagram. The Simulink fixed-point model is illustrated in Figure 4. The frequency-response of the RRC filter is illustrated in Figure 5. The FPGA utilization for the PN DDOR generation system relative to the baseline IRIS FPGA build (build without PN DDOR functionality) is listed in Table 1. We note that the majority of required multipliers are due to the RRC transmit filter/interpolator. It may be possible to further optimize this pulse-shaping filter by utilizing canonical-signed-digit (CSD) representation for the filter coefficients, but no effort was done in this regard.

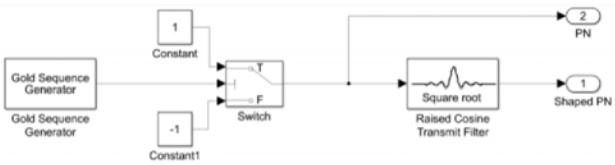

Figure 4: Simulink fixed-point model.

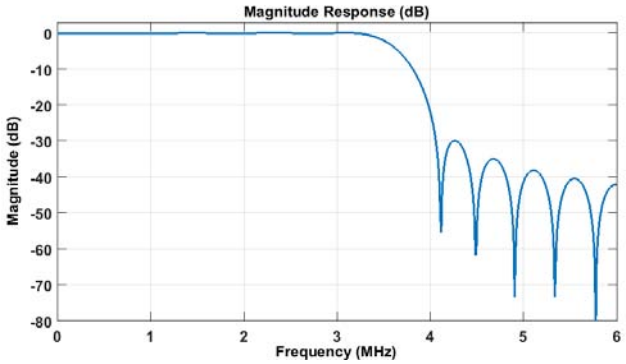

Figure 5: Frequency response for fixed-point RRC filter.

Table 1: Summary of FPGA utilization for PN DDOR system.

Category	Increase in FPGA Utilization Relative to Baseline Design (PN DDOR Module Only)	Increase in FPGA Utilization Relative to Baseline Design (PN DDOR and Pre-distortion Filter)
Slice Registers	1.38%	13.93%
Slice LUTs	1.10%	8.01%
Logic LUTs	0.99%	7.90%
DSP48E	0.00%	77.66%

The generated block was integrated to the Iris firmware and additional modes were created to enable normal Iris operation, including classical DDOR modes, as well as the newly implemented PN DDOR mode.

However, upon performing frequency-domain verification of the output spectrum, it was observed that the IRIS radio output spectrum (being initially designed for relatively low data rate communication) experiences significant shaping at the high frequencies where the PN DDOR signal is generated. For this reason, a digital pre-distortion filter was implemented in order to flatten the final spectrum produced by the IRIS radio. The FPGA utilization including this pre-distortion filter is listed in the final column of Table 1. Observe that the increase in complexity is due to the use of a 129-tap FIR filter (which utilizes fixed-point multipliers through the DSP48E FPGA blocks) for the pre-distortion shaping. This filter was not optimized for FPGA utilization, such as utilizing a CSD approach to the filter coefficients. We emphasize that the numbers listed in Table 1 are relative utilization numbers. The true gate/DSP48E block utilization on the Virtex-6 FPGA remains relatively low [2-3].

What remains is the time-domain verification of the output of the Iris X-band downlink. This output should correlate well to the Gold code implemented onboard the Iris radio. In the next section, we will record the output of the Iris radio, which will allow us to perform offline processing to recover the code and to verify the autocorrelation result.

4. Time-domain Verification of Iris Output

The time-domain verification of the Iris radio output was performed by capturing the X-band wide-band signal via test-equipment. The captured signal is then demodulated to verify the code structure output by the radio. We utilized a Keysight spectrum analyzer to capture I/Q samples of the X-band output of the Iris flight unit. The demodulation of the recorded signal is necessary. This procedure is illustrated in Figure 6, and includes a frequency recovery stage, a timing-recovery loop, and finally hard-thresholding.

Figure 6: Software-receiver architecture for demodulation of recorded Iris output.

This receive chain was implemented in MATLAB using tools from the communication toolbox. The phase estimates from the PLL as well as the soft symbols are illustrated in Figure 7. We observe that the soft symbols are generally very far away from the threshold (zero) and thus are not likely to yield bit errors once hard decisions are made.

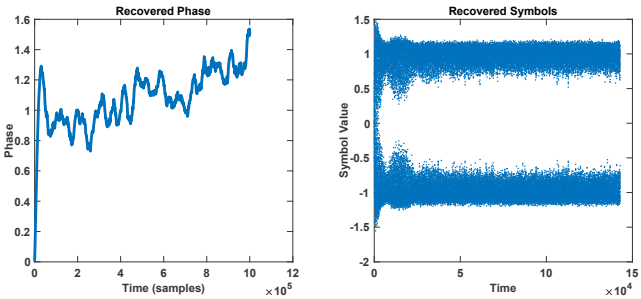

Figure 7: Recovered phase and soft-symbols from recorded data.

The correlation of the hard decision bits from the soft-symbol output illustrated in Figure 7 against the true Gold code is illustrated in Figure 8. We observe that the maximum correlation value for all the peaks except the truncated ones is exactly $2^N - 1$ (the length of the code) and thus the signal was correctly demodulated to confirm the presence of the valid code. We stress, however, that our verification procedure for the Iris implementation and is not intended to be a reference DSN implementation, which is likely to consider many other effects in the DDOR calculations.

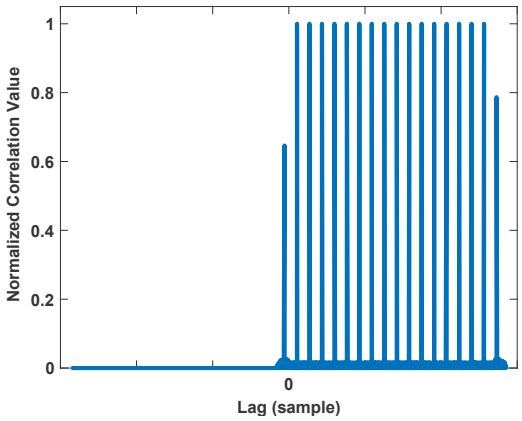

Figure 8: Normalized correlation of time and frequency compensated received samples against true Gold code.

5. Future Work and Conclusions

Now that PN DDOR mode has been successfully demonstrated on an Iris radio flight unit, the following tasks are being considered: First, we plan on implementing the X-band PN DDOR on the Universal Space Transponder (UST). Active discussion is in the work with the UST team in order to implement the PN DDOR mode on the UST prototype radio. One characteristic of the UST that may cause the design to differ to due to the different implementation of UST compared to Iris is the FPGA frequency.

Second, we hope to infuse the X-band PN DDOR mode onto one or two of the Iris EM-1 radios flight software. This will provide an opportunity to demonstrate the PN DDOR mode in flight in the near future. A proposal is being prepared to consider infusing the PN DDOR mode into the two EM-1 missions: Lunar Flashlight and NEAScout. We hope that such infusion will allow us to perform more rigorous testing of the PN DDOR subsystem, including possibly through the use of the Block V receiver.

Finally, we plan on extending the X-band design into the Ka-band. Requirements are being prepared for the Ka-band version of the PN DDOR mode. Next, a suitable Gold code and an appropriate RRC filter will be tailored to the Iris and/or UST proposed Ka-band designs. These codes and RRC filters can be obtained by following the design methodology outlined in Sec. 2.

6. Acknowledgements

We would like to graciously thank Faramaz Davarian (member of the Communication Technologies and Standards Program office at JPL) for providing funding this effort. Faramaz also provided many valuable suggestions through discussions that helped improve this work and manuscript. We also would like to thank the Iris team, including Brandon Burgett, Sarah Holmes, and Lauren McNally for making an Iris prototype available for testing and evaluations.

7. References

[1] Delta-DOR—Technical Characteristics and Performance. CCSDS Green Book 500.1-G-1. May 2013.

[2] M. M. Kobayashi, T. Dobreva, E. Satorius, S. Holmes, A. Yarlagadda, F. Aguirre, M. Chase, K. Angkasa, B. Burgett, and L. McNally, "The Iris Deep-Space Transponder for the SLS EM-1 Secondary Payloads," Submitted for publication.

[3] M. M. Kobayashi, "Iris Deep-Space Transponder for SLS EM-1 CubeSat Missions," in 2017 Small Satellite Conference, Logan, Utah, Aug. 2017, pp.1-7.

[4] B. P. Lathi, Z. Ding. Modern Digital and Analog Communication Systems, 4th edition. Oxford University Press. Page 674.

[5] R. Gold, "Optimal binary sequences for spread spectrum multiplexing (Corresp.)," in IEEE Transactions on Information Theory, vol. 13, no. 4, pp. 619-621, October 1967.

[5] New Wave Instruments, Linear Feedback Shift Registers. http://www.newwaveinstruments.com/resources/articles/m_sequence_linear_feedback_shift_register_lfsr.htm. Retrieved May 10th, 2018.

Biography

Zaid Towfic *holds a B.S. in Electrical Engineering, Computer Science and Mathematics from the University of Iowa. He received his Electrical Engineering M.S. in 2009 and Ph.D. in 2014, both from UCLA, where he focused on signal processing, machine learning, and stochastic optimization. After receiving his Ph. D., Zaid joined the MIT Lincoln Laboratory where he worked on distributed beam forming and geolocation, interference excision via subspace methods, simultaneous communication, and electronic warfare. Zaid joined the Jet Propulsion Laboratory in January of 2017 and has been focused on machine learning and signal processing efforts.*

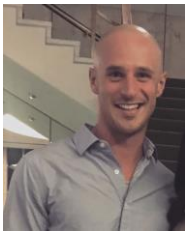

Thaddaeus Voss *received his B.S. (2015) from the University of Cincinnati and his M. S. (2017) from the University of Southern California in Electrical Engineering. He joined the Jet Propulsion Laboratory in 2018 where he is a Signal Analysis Engineer in the Communications Systems Engineering group. During his time at JPL he has supported the development of the NISAR UST Ka-band Modulator and the Iris Deep-Space Transponder.*

Mazen Shihabi *holds B.S. and M.S. from University of Southern California, and PhD from University of California at Irvine, all in Electrical Engineering with emphasis on digital communications. He joined the Jet Propulsion Laboratory (JPL) in 1990 as a member of the Communications Research Section where he worked on modem design, bandwidth efficient modulations, and arraying techniques applicable to flight and ground communication systems. From 1996 to 2008, he worked in the commercial sector on telecom technologies related to aerospace, cellular service, and remote patient monitoring. Dr. Shihabi rejoined the JPL, Flight Communications Section in 2008 where he has supported software defined radio technology for flight projects and flight technology demonstrations. Since 2011 Mazen has been the technical and operations lead for the MRO relay telecom subsystem that provides prime relay support to the Mars Science Lander. Mazen was instrumental in preparing, ground testing, and demonstration of software and firmware upgrades to the MRO flight radio, in-situ at Mars, to support high rate and Automated Data Rate (ADR) relay support to the MSL mission. Currently, Mazen is the Group Supervisor of the Communications Architecture and Operations focusing on new communications technologies and services.*

James Border *received his B.A in physics from the University of Iowa in 1974 and Ph.D. in Mathematics from U.C. San Diego in 1979. He has been with JPL for more than 37 years and is an expert in analysis of radiometric data and applications of VLBI to spacecraft navigation. He lead development of the Deep Space Network ground data system to enable high accuracy spacecraft angular position measurements. His responsibilities have included system engineering, receiver design, signal processing algorithm development, error analysis, and development of calibration techniques to improve accuracy.*